Experimental Demostration of a MIMO-OFDM Underwater Optical Communication System for Reducing Alignment Angle Requirements

Boxun Li, Min Fu, Mengnan Sun, Xuefeng Liu, and Bing Zheng, *Member, IEEE*

***Abstract*—Although the underwater optical communication system (UWOC) plays an important role in many marine applications, the acquisition, pointing and tracking (APT) problems are still great challenges in a long or turbid water channel. The Orthogonal Frequency Division Multiplexing (OFDM) and the space-time block coding (STBC) technologies have been introduced in UWOC systems to improve spectral efficiency and data transmission reliability. On these foundations, a multi-input multi-output (MIMO) mode is proposed and verified in this article to reduce the alignment requirement. In experiments, two sets of 450 nm blue laser diodes (LDs) and PIN photodiodes are selected as light sources and receivers, and then parallel light beams are generated and modulated using an Alamouti coding for its anti-interference ability. The receiving plane is rotated to simulate the various alignment situations, and the system performance of MIMO-OFDM and single-input single-output OFDM (SISO-OFDM) are compared in tap water and turbid water. The results show that the spatial diversity in MIMO can extend the communication range and its single-sided maximum detection angle range is 92% and 112% higher than the SISO system, respectively.**

***Index Terms*—Alignment, APT, MIMO-OFDM, STBC, UWOC.**

I. Introduction

THE vast ocean contains a variety of rich resources, and ocean exploration has become an inevitable trend of historical development. To support various ocean applications such as underwater navigation and underwater wireless sensor networks (UWSNs), high-bandwidth data transmission through Underwater Wireless Communication Technologies (UWCTs) is essential. For UWOC, the attenuation coefficients of different types of water vary significantly depending on the wavelength of light, with longer attenuation lengths observed for wavelengths between 450 nm and 550 nm [1]. The discovery of this window of blue-green light propagation holds great significance for the advancement of UWOC. The advantages of UWOC technology include large modulation bandwidth, high transmission rate, small transceiver equipment, and relatively low power consumption. It is typically used for underwater sensing and monitoring tasks such as underwater imaging and marine life observation. The potential applications of UWOC technology are extensive and could offer significant benefits to various industries and scientific disciplines.

In UWOC systems, Laser diodes (LDs) and Light Emitting Diodes (LEDs) are usually used as light sources. The modulation bandwidth of LEDs is usually limited to several MHz, making high-speed communication impossible. Although LEDs have a large divergence angle and can spread over large areas, they can only support short transmission distances in water environments with high turbidity. LDs with high modulation bandwidth and concentrated energy are often used for long-distance, high-speed communications. These works use LD as the light source in the experiment [2], [3], [4], [5], [6], [7], [8], [9], [10], [11], [12], [13]. Shen et al. reported a 20 m/1.5 Gbps UWOC system based on a 450 nm laser diode (LD) transmitter with a non-return-to-zero on-off-keying (NRZ OOK) signal [2]. In addition, advanced modulation schemes, such as OFDM and Pulse Position Modulation (PPM), are commonly used in UWOC systems. These schemes can enhance spectral efficiency and increase data transmission rates. A data rate of 9.6 Gbps over an 8 m transmission distance was reported by a 405 nm blue-light LD transmitter using 16-quadrature amplitude modulation Orthogonal Frequency Division Multiplexing (QAM-OFDM) modulation scheme [3]. Zhao et al. achieved a UWOC system using a 3×1 fiber combiner to extend the transmission distance, and a maximum transmission distance of 100 meters is achieved at a data transmission rate of 8.39 Mbps in a standard swimming pool [14].

Despite the many advantages of UWOC, there are still many challenges. The underwater environment is intricate, and the existence of particles in seawater causes absorption and scattering effects, which diminish the optical power received. The above works primarily focused on the line-of-sight (LOS) configuration, which require strict coaxiality between the transmitter

Manuscript received 18 November 2023; revised 16 January 2024; accepted 17 January 2024. Date of publication 22 January 2024; date of current version 19 February 2024. This work was supported in part by Key Research and Development Projects in Hainan Province under Grant ZDYF2022GXJS001, in part by Shandong Provincial Natural Science Foundation under Grant ZR2020MF011, and in part by the Hainan Province of China under Grant ZDKJ202017. *(Corresponding author: Min Fu.)*

Boxun Li and Mengnan Sun are with the College of Electronic Engineering, Ocean University of China, Qingdao 266100, China (e-mail: lbx19980015@163.com; sunmengnan@ouc.edu.cn).

Min Fu and Bing Zheng are with the College of Electronic Engineering, Ocean University of China, Qingdao 266100, China, and also with Sanya Oceanographic Institution, Ocean University of China, Sanya 572024, China (e-mail: fumin@ouc.edu.cn; bingzh@ouc.edu.cn).

Xuefeng Liu is with the College of Automation and Electronic Engineering, Qingdao University of Science and Technology, Qingdao 266061, China (e-mail: snowclub@qust.edu.cn).

Digital Object Identifier 10.1109/JPHOT.2024.3356723

and receiver side of the communication. But the presence of underwater turbulence can cause optical flicker and beam drift, making alignment more difficult. Therefore, before the UWOC system can be applied in real underwater environments, APT problems need to be addressed and resolved, which is the premise of establishing underwater laser communication [15]. In the field of visible light communication (VLC), several APT systems have been proposed and experimentally verified. These systems can be categorized into two main categories: APT methods based on received-signal-strength-indicator (RSSI) and visual-based APT methods. The RSSI-based APT system employs an optical sensor to detect signal strength and utilizes three anchors to determine its position through standard trilateration. In 2016, an efficient transceiver auto-alignment and tracking scheme has been proposed for practical VLC and laser-based free-space optical communication (FSO) systems [16]. This scheme utilizes a transceiver that is developed based on field-programmable gate array (FPGA), and combines auto-alignment and tracking functionalities. It successfully demonstrates real-time transmission of 200 Mbps amplitude phase modulation (CAP) over a dynamic 3-meter VLC link. In 2021, Lin et al. proposed an APT system to solve problems related to UWOC mobility, and studied the impact of the underwater environment on the APT system for the first time [17]. When the UWOC transmitter and receiver were in relative motion, they achieved Re-adjust the system attitude within 0.04 seconds.

As the advantages of MIMO technology become increasingly apparent, researchers have begun to apply it to the field of VLC. In [18], Jim et al. proposed an underwater optical communication system based on space diversity technology. It is verified that in water environments with strong scattering effects, space diversity technology can reduce fading at the receiver. In [19], Ahmad et al. implemented an imaging visible light communication system with a communication rate of 1 Gbps at a communication distance of 1 m using the MIMO-OFDM method. The system consists of 4 transmitters and 9 pixel imaging receivers, with a communication rate of 250 Mbps for each transmitted signal. In [20], Chen et al. implemented non-Hermitian symmetric OFDM modulation mode and angle diversity reception technology in MIMO system to determine the effective coverage area of communication. The conclusion shows that the light distribution is mainly determined by the specific location of the LED installation and the peak brightness of the LED. In MIMO systems, space-time coding is widely used. Space-time coding can be divided into two categories: Space Time Block Code (STBC) and Space Time Trellis Code (STTC). The main advantage of STBC is that maximum diversity gain can be obtained and relatively simple linear processing is required at the receiver. By utilizing STTC, the coding gain can be improved. Spacing-time coding techniques are commonly employed to reduce the impact of deep fading and intensity fluctuation caused by optical turbulence in underwater environment. In cooperative FSO systems, a high-order intensity modulation orthogonal STBC scheme is proposed [21], which can mitigate inter-symbol interference (ISI) and provide diversity gain in MIMO systems. But none of these works took the alignment angle problem into consideration. In [22], Song et al. established a 2×2 MIMO-OFDM system using repetition coding (RC) and Alamouti space-time block coding (STBC) schemes, and conducted experiments under different turbidity. Guo et al. proposed a STBC MIMO visible light communication scheme based on precoding, which minimized the bit error ratio (BER) without changing the transmit power [23].

One of the promising solutions to solve the alignment problem is STBC technology. Alamouti coding is a less complex STBC scheme applied to MIMO systems. In the Alamouti scheme, two independent antennas are used to send two versions of the signal, allowing multiple copies of the signal to be used to reconstruct the original signal at the receiver. Even if parts of the signal path are not precisely aligned, the communication system can still ensure signal transmission quality. Underwater optical communication channels exhibit nonlinear characteristics, and the structure of Alamouti coding enables the communication system to resist this nonlinear effect to a certain extent. In addition, due to the orthogonal nature of Alamouti encoding, the receiving end can use relatively simple decoding algorithms to process signals. Compared with other more complex coding technologies, Alamouti coding can significantly reduce the computing resources and processing time required to process signals, making the entire communication system more efficient and practical.

In this article, a 2×2 MIMO-OFDM UWOC system is constructed, which incorporates space diversity and the Alamouti coding scheme to minimize the alignment angle requirement. This study conducts experiments to measure the communication range of the MIMO-OFDM system employing the STBC scheme and the SISO-OFDM system. The results show that the single-sided detection range of the MIMO system is increased by 92% in clear water and 112% in turbid water compared with the SISO system.

II. Principles

The complex orthogonal space-time code for two transmitting antennas was proposed by Alamouti [24]. In the Alamouti scheme, two consecutive symbols x1 and x2 are encoded according to the space-time code matrix as shown in (1). In the first symbol cycle, two symbols x1 and x2 are transmitted simultaneously from two antennas, respectively. In the second symbol cycle, both symbols are emitted again, with one antenna emitting $-x_2^*$ and the second one emitting $x1^*$. The encoding matrix can be expressed as:

$$X = \begin{bmatrix} x_1 & -x_2^* \\ x_2 & x_1^* \end{bmatrix} \tag{1}$$

The coding matrix uses the orthogonal design principle,

$$\begin{aligned} X * X^H &= \begin{bmatrix} |x_1|^2 + |x_2|^2 & 0 \\ 0 & |x_1| + |x_2|^2 \end{bmatrix} \\ &= (|x_1|^2 + |x_2|^2) I_2, \end{aligned} \tag{2}$$

where I_2 is a 2×2 unit matrix. When consider only one receiving antenna, the received signal can be described as

$$y_1 = h_{11}x_1 + h_{21}x_2 + n_1, \tag{3}$$

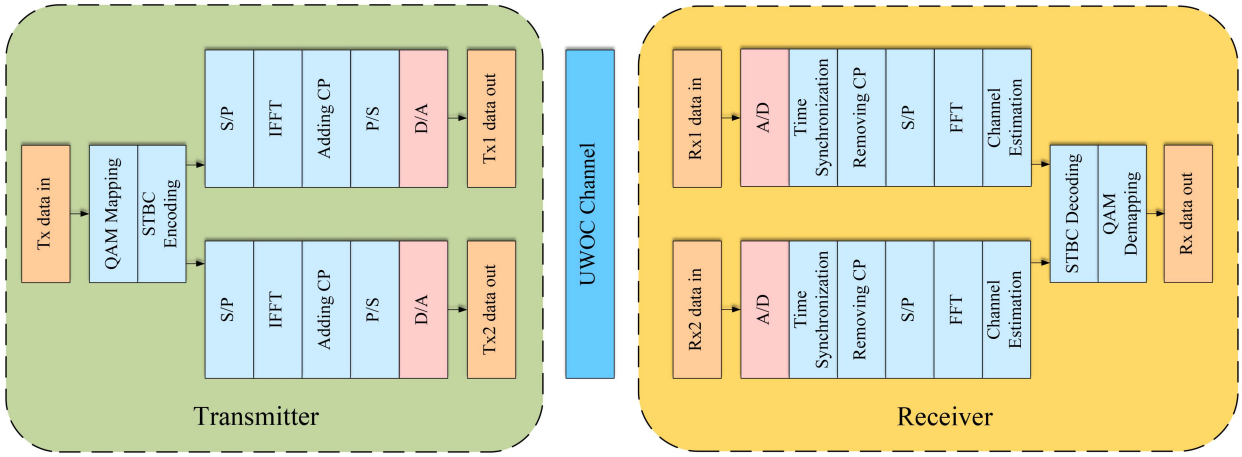

Fig. 1. Block diagram of the STBC-based MIMO-OFDM UWOC system.

$$y_2 = h_{12}\left(-x_2^*\right) + h_{22}x_1^* + n_2, \tag{4}$$

where h_{ij} is the i-th transmitter and the j-th symbol period, n_i is the additive noise of the i-th symbol period. Signal detection uses the maximum likelihood estimation algorithm. Assuming that when the channel gain of two symbol periods remains unchanged, that is, $h_{11} = h_{21}$, $h_{21} = h_{22}$, the estimation result of the detected signal can be described as

$$\hat{x}_1 = h_{11}^* y_1 + h_{12} y_2^* = \left(|h_{11}|^2 + |h_{12}|^2\right) x_1 + h_{11}^* n_1 + h_{12} n_2^*, \tag{5}$$

$$\hat{x}_2 = h_{12}^* y_1 - h_{11} y_2^* = \left(|h_{11}|^2 + |h_{12}|^2\right) x_2 - h_{11} n_2^* + h_{12}^* n_1. \tag{6}$$

In an OFDM system, the bandwidth is divided into multiple subcarriers, with each subcarrier functioning as an independent channel. To ensure a precise channel matrix, channel estimation is conducted for each OFDM data subcarrier during the experiment.

III. Experimental Description

A. Experimental Setup

The transmitter first generates a sequence of random bits in Matlab, which are then mapped by quadrature amplitude modulation (QAM) and input into the space-time encoder to convert the data stream into two parallel streams. Inverse fast Fourier transform (IFFT) with Hermitian symmetry is employed to generate a real-valued OFDM signal. A cyclic prefix (CP) is added to each OFDM data symbol to mitigate the effects of intersymbol interference (ISI). The system architecture is shown in Fig. 1. The OFDM signal parameters of the system are set as follows: an IFFT size of 128, the data subcarrier number of 52, a CP length of 16, and a frequency gap of 2 subcarriers near zero frequency. After transmission through the underwater channel, the optical signal is received by the PIN photodetector. The signal undergoes symbol synchronization, channel estimation, OFDM demodulation, and recovery of the binary bit sequence through space-time decoding and QAM de-mapping. The system achieves a total data rate of 131.3 Mbps.

At the transmitter side, two signals are loaded into an arbitrary waveform generator (AWG) and the digital-to-analog conversion rate is set to 100 MSample/s. To fully utilize the modulation performance of LD and maintain the signal within its modulation range, the output signal is amplified by an amplifier (Mini-Circuits ZHL-6A-S+) and adjusted in amplitude by variable electrical attenuators (VEAs, attenuation range: 0-30 dB). The attenuation value in this system is 17 dB. Following the loading process, the signal is loaded to a 450 nm blue laser diode through a Bias-Tee (Thorlabs LDM38/M), which is accompanied by a laser controller (Thorlabs LDC205 C) and a temperature controller (Thorlabs TED200 C). The bias current of the laser diode is set to 75 mA, the output optical power is 80 mw, and the operating temperature is set to 25 °C to make the LD work under suitable conditions. The PIN photodetector (Thorlabs PDA10A2) has a small bandwidth of 150 Mhz, a wavelength detection range of 200 to 1100 nm and an active area of 0.8 mm^2. The received optical signal is converted into an electrical signal by the PIN. The amplitude of the electrical signal is then adjusted through the use of an amplifier and an attenuator. The arrangement of the above experimental setup is illustrated in Fig. 2. Subsequently, the received signal is captured by a digital oscilloscope and then transmitted to a computer for demodulation.

B. Experimental Procedure

This study presents an experimental demonstration of a 2×2 MIMO-UWOC system that utilizes STBC scheme to simplify alignment problem. After the signal is modulated onto the light source and sent out, the light signals passing through the underwater channel are detected by photodetectors. The received signals are processed in analog/digital conversion (A/D) and handed over to the computer for demodulation. To simulate an underwater channel, an experiment is conducted using a water tank measuring 2.4 m in length, 0.35 m in width, and 0.35 m in height. As is shown in Fig. 3, the deflection angle θ of the receiving plane increases gradually from 0 degrees, increasing

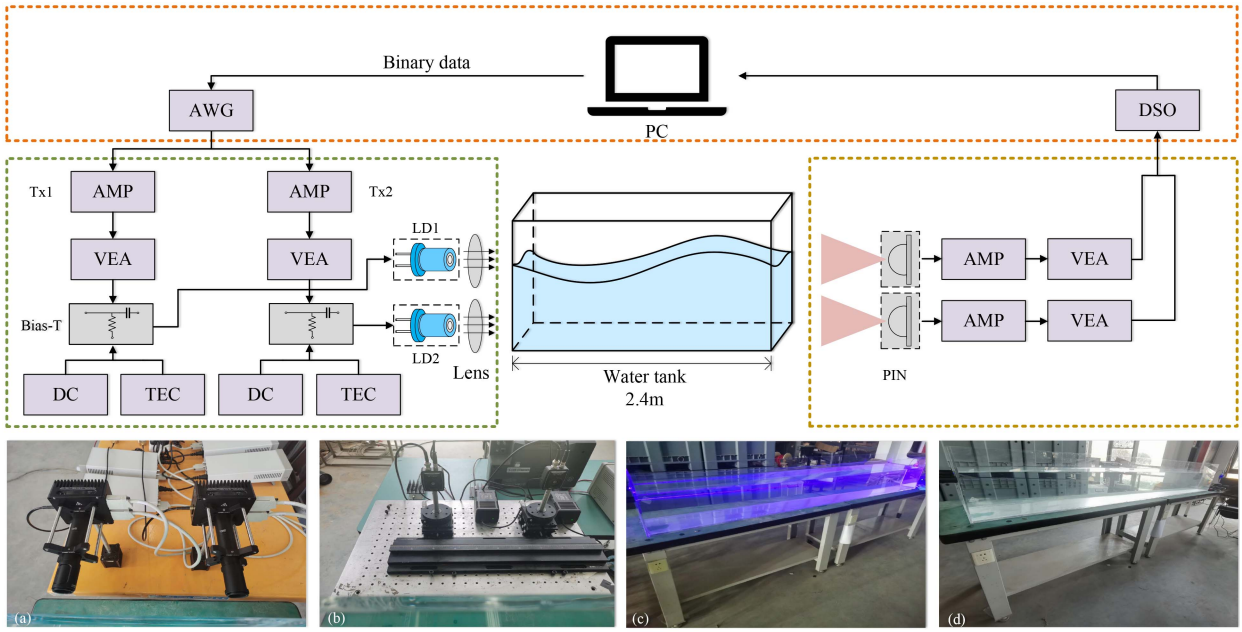

Fig. 2. Experimental setup of STBC-based 2×2 MIMO-OFDM UOWC system. (a) Transmitters. (b) Receivers. (c) 2.4 m water tank. (d) Underwater channel at an attenuation factor of 0.5713 m^{-1}.

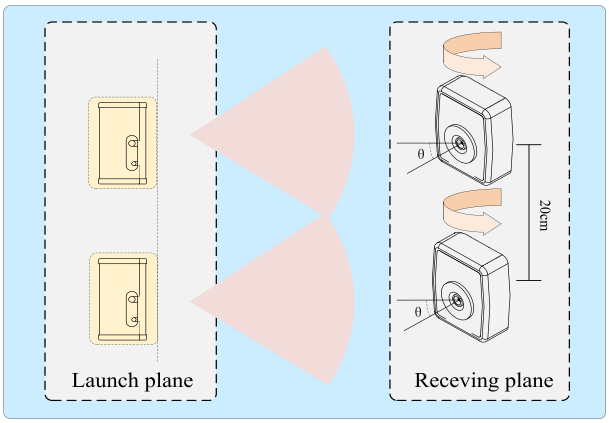

Fig. 3. Architecture of the STBC-based MIMO-OFDM UWOC system.

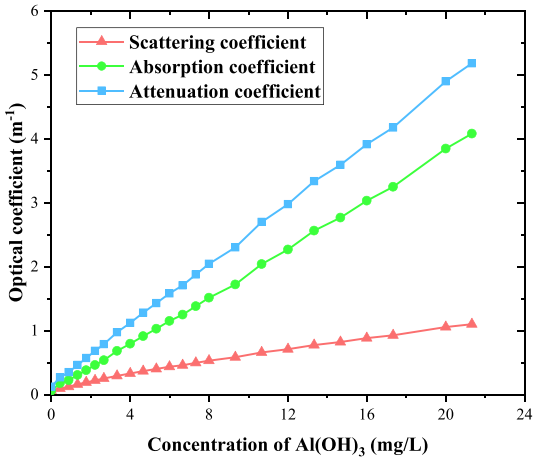

Fig. 4. Attenuation coefficient as a function of $Al(OH)_3$ concentration.

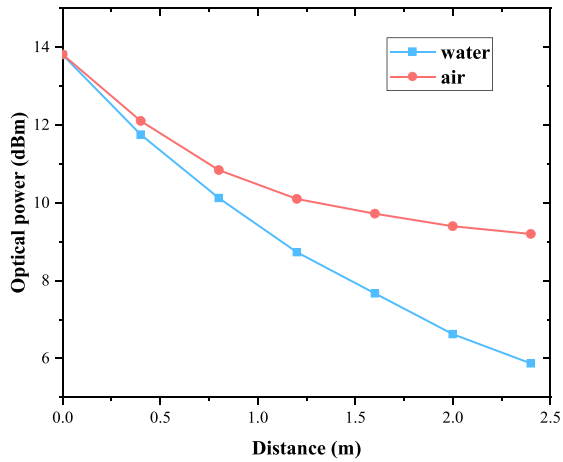

Fig. 5. Received optical power in water and air as a function of distance.

by 10 arcmin each time. After the bit sequence is recovered from the received signal, the BER is calculated.

The underwater environment is known for its complexity, and light beam transmission in water can be influenced by various factors, including absorption and scattering effects. These works involve the modification of water's optical properties through the addition of powder [25], [26]. In [25], Guo et al. changed the absorption coefficient, scattering coefficient and attenuation coefficient level of water by adding $Al(OH)_3$ powder.

In this experiment, two photodetectors, positioned 20 cm apart from each other at the center of the light spot, initially parallel to the plane of the transmitter and are subsequently deflected by a 360° rotating displacement table. The light beams are directed onto the light-receiving surface of the detectors. In order to

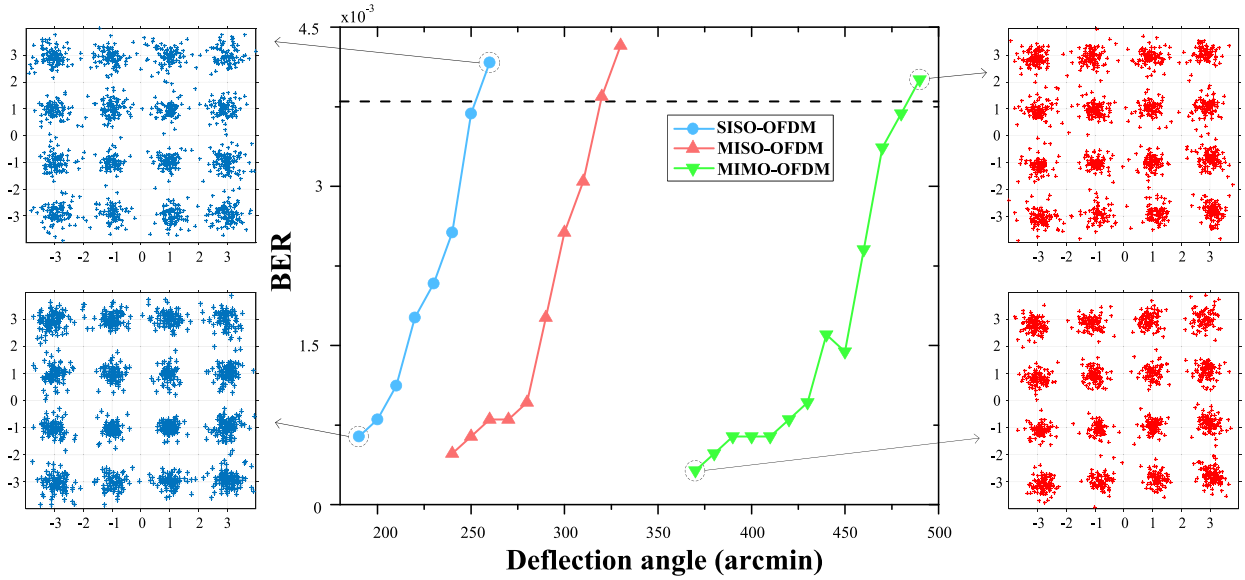

Fig. 6. BER performance at different deflection angles in clean water.

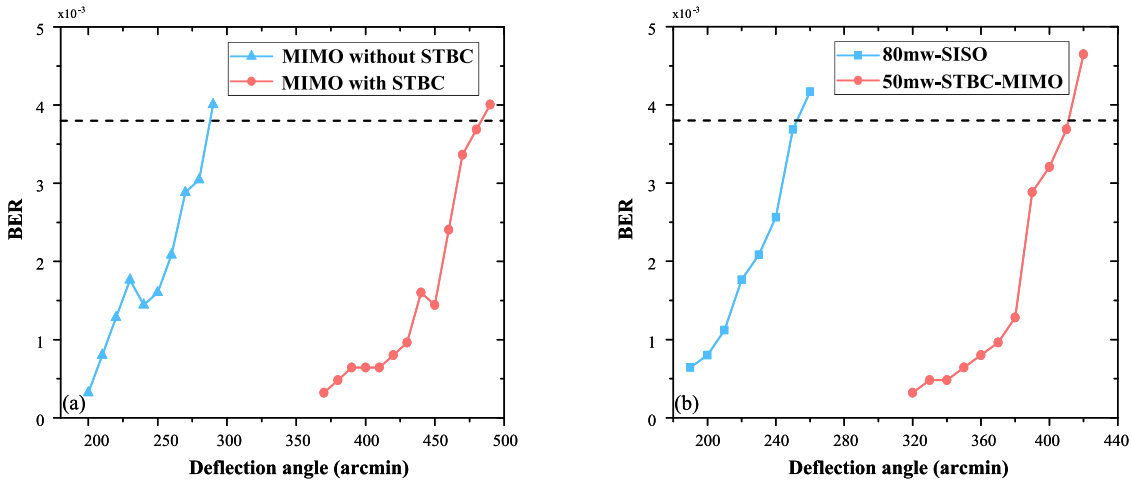

Fig. 7. (a) BER performance with and without STBC encoding. (b) BER performance under different optical powers at different deflection angles.

maintain consistency in the total optical power of two beams, an optical attenuator is installed at the transmitter.

The experiments are conducted in two types of water environments: clear water and turbid water. Water attenuation at different dopant concentrations is measured. In order to ensure the reliability of the data, all measurements are completed in the water tank where the experimental equipment is located. Before measurement, in order to reduce errors that may be introduced by direct measurement, the measuring equipment needs to be calibrated with pure water. Start by immersing the device completely in the water, making sure to remove the air. Afterwards, ensure normal operation of the equipment within a 15-minute measurement period, and use the data at a wavelength of 450 nm as the calibration benchmark from the obtained data. In the experiment, an electronic scale is used to weigh different doses of dopants each time to prepare solutions of different concentrations. Ensure that the orientation and location of the device as well as the voltage and current are consistent for each measurement. Through multiple measurements, the water attenuation coefficient under different dopant concentrations at 450 nm wavelength can be obtained. The study initially focused on tap water as the experimental environment, with a measured water attenuation coefficient of 0.1222 m^{-1}. The detection angle ranges of MIMO-OFDM, MISO-OFDM and SISO-OFDM systems are experimentally investigated and compared, with other experimental conditions held constant. After that, the powder is gradually added to water, and continue to conduct the experiment at an attenuation coefficient of 0.5713 m^{-1}. The consistency of experimental results is observed to determine whether the STBC-MIMO scheme can reduce the alignment angle requirements, by comparing the results of the two experiments.

IV. Result and Discussion

In order to simulate the real water environment in the experiment, different weights of powder are added to the water, and the attenuation coefficient at different $Al(OH)_3$ concentrations was measured by the absorption attenuation tester (WETLabs

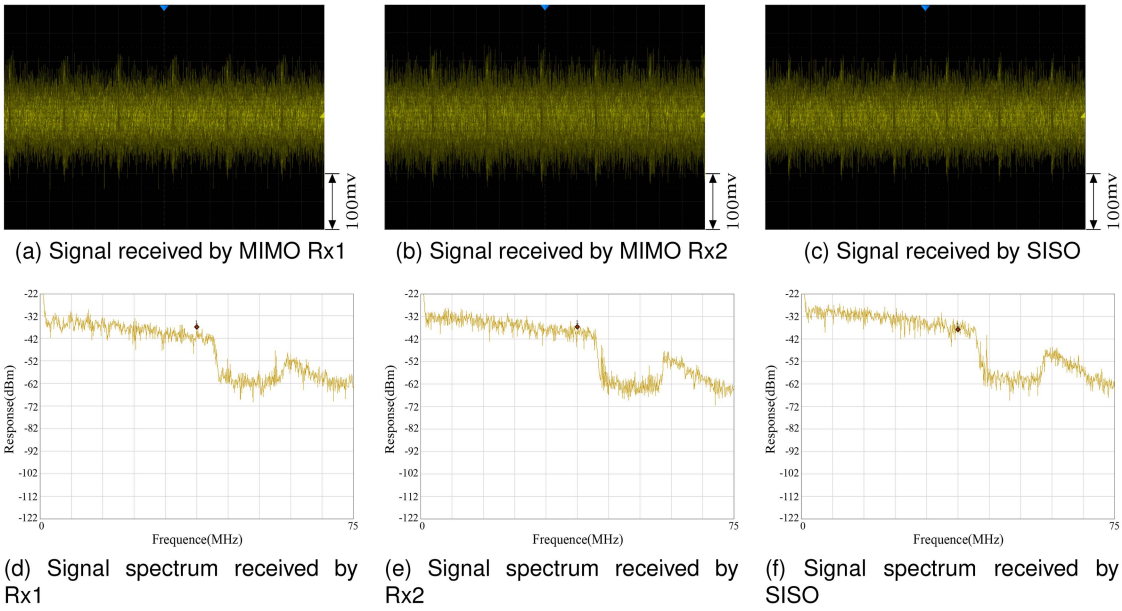

Fig. 8. MIMO-OFDM and SISO-OFDM signals and spectrum received in tap water when the light reaches the receiving plane vertically.

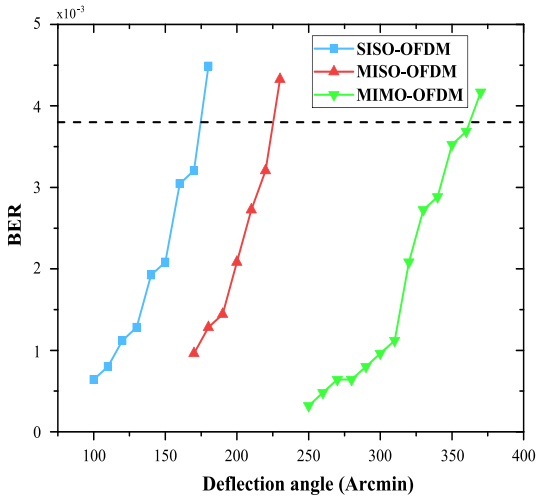

Fig. 9. BER performance at different deflection angles in turbid water.

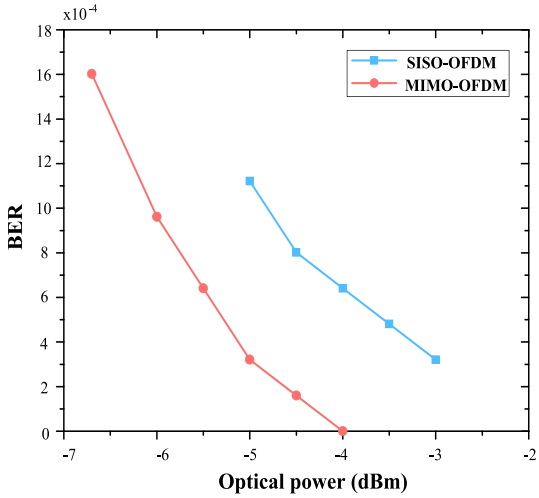

Fig. 10. BER performance under different received optical power.

AC-S). In the experiment, the attenuation coefficient is used to measure the turbidity of the water environment. Fig. 4 shows the attenuation coefficients for different powder concentrations at a wavelength of 450 nm. Furthermore, in order to obtain an appropriate optical transmission distance, we conducted an estimation of the light intensity loss resulting from the divergence angle of the laser spot. To do this, a continuous beam of blue light was transmitted into air and clear water, and then the optical power at different transmission distances was measured using an optical power meter. The optical power at different transmission distances is shown in Fig. 5. When the spot of the beam expands with increasing distance, the same light power is distributed over a larger area, resulting in a decrease in light intensity per unit area.

In the experiment, $Al(OH)_3$ powder was first added to the water to make the attenuation coefficient become 0.1222 m^{-1}. Fig. 6 illustrates the BER performance of three types of OFDM signals, namely SISO-OFDM, MISO-OFDM, and MIMO-OFDM diversity signals, at varying deflection angles, which provides a comparison of the reduced alignment performance of each signal type in this environment. In the case where the BER is below the forward error correction (FEC) threshold, the STBC-MIMO scheme can detect angles up to a maximum of 480 arcmin, which is 54% and 92% wider than that of STBC-MISO and SISO-OFDM schemes. In order to investigate the role of STBC in reducing alignment angle requirements, experiments were conducted on MIMO systems with and without STBC coding. Fig. 7(a) illustrates that the detection range is significantly improved after adding STBC encoding. On the other hand, to ensure that the increase in detection angle of the STBC-MIMO system compared to the SISO system is not solely attributed to a simple increase in optical power, we conducted a comparison of the detection ranges under different transmit optical powers. Under the current experimental environment and on the premise that the laser

diode can work normally, the transmit optical power of each transmitter of the MIMO system is reduced to 50 mw, and the transmit power of the SISO system remains unchanged. Fig. 7(b) illustrates that even when the transmitted optical power is lower than that of the SISO system, the STBC-MIMO system still exhibits superior performance. Fig. 8 shows the time domain waveform and spectrum of the signal in tap water at the center of the receiving plane. The DC component and virtual subcarriers are clearly visible in the spectrum.

In turbid water, the light beam is greatly affected by absorption and scattering effects. To investigate whether the STBC-MIMO system still has lower alignment requirements in different water environments, additional experiments were carried out in a water environment with an attenuation coefficient of 0.5713 m^{-1}, and all other conditions were kept constant. In Fig. 9, the STBC-MIMO scheme is capable of detecting single-sided angles up to 360 arcmin, and this range is 64% and 112% wider than that of the STBC-MISO and SISO-OFDM schemes respectively. Therefore, based on the experimental results, it can be concluded that the MIMO-OFDM system requires lower alignment, which ultimately enhances the performance of the UWOC system.

To further analyze the impact of optical power attenuation on system performance, the powder concentration was gradually increased in the experiment, resulting in a gradual decrease in the received optical power. The light spot is located at the center of the receiver, the transmission distance is fixed at 2.4 m, and other experimental conditions remain unchanged. The relationship between the BER of two UWOC systems and the received optical power can be shown in Fig. 10. Compared with the SISO system, under the FEC threshold, the minimum received optical power of the MIMO system is increased by 2 dBm, which indicates that the MIMO system can transmit a longer distance under the same optical power. According to the conducted experiments, the MIMO-OFDM system achieves diversity gain through spatial diversity, which increases the range of detection and reduces the need for precise alignment in intricate water environments. Due to the limitations of the water tank and the experimental setup, no additional MIMO light paths were conducted. As the scale of the MIMO system increases, the number of antennas in the system also increases. This leads to finer signal differentiation and more complex data modulation. Consequently, the achieved diversity gain also increases, resulting in better signal quality at the receiving end. This improved signal quality allows for a wider range of alignment angles.

V. Conclusion

In this article, a 2×2 MIMO-OFDM UWOC system is proposed to reduce the alignment angle requirements. The proposed system uses Alamouti coding to obtain diversity gain and achieves underwater 2.4 m transmission with a data rate of 131 Mbps. In a tap water environment with an attenuation coefficient of 0.1222 m^{-1}, the 2×2 MIMO-OFDM system can detect signals at a maximum angle of 480 arcmin, while the SISO-OFDM system can detect signals at a maximum angle of 250 arcmin. Additionally, when experimented in turbid water with an attenuation coefficient of 0.5713 m^{-1}, the detection range of the MIMO system is up to 360 arcmin, which is 112% wider than that of the SISO system. The study confirms that the UWOC system using the STBC-MIMO scheme can reduce the need for precise alignment in underwater communication links and can be applied in situations where alignment is challenging. This system uses space diversity technology to enhance the reliability of the communication system at the cost of the communication rate. The MIMO diversity technique offers a new approach to addressing APT problems. Its advantages, including relaxed alignment requirements and the ability to communicate over relatively long distances, make it a practical significant solution for the development of underwater optical communication.

References

[1] S. Q. Duntley, "Light in the sea," *J. Opt. Soc. Amer.*, vol. 53, no. 2, pp. 214–233, 1963.

[2] C. Shen et al., "20-meter underwater wireless optical communication link with 1.5 Gbps data rate," *Opt. Exp.*, vol. 24, no. 22, pp. 25502–25509, 2016.

[3] H.-H. Lu et al., "An 8m/9.6 Gbps underwater wireless optical communication system," *IEEE Photon. J.*, vol. 8, no. 5, pp. 1–7, Oct. 2016.

[4] X. Chen, W. Lyu, Z. Zhang, J. Zhao, and J. Xu, "56-m/3.31-Gbps underwater wireless optical communication employing Nyquist single carrier frequency domain equalization with noise prediction," *Opt. Exp.*, vol. 28, no. 16, pp. 23784–23795, 2020.

[5] J. Wang, C. Lu, S. Li, and Z. Xu, "100m/500 Mbps underwater optical wireless communication using an NRZ-OOK modulated 520nm laser diode," *Opt. Exp.*, vol. 27, no. 9, pp. 12171–12181, 2019.

[6] J. Wang et al., "Underwater wireless optical communication based on multi-pixel photon counter and OFDM modulation," *Opt. Commun.*, vol. 451, pp. 181–185, 2019.

[7] S. Hu, L. Mi, T. Zhou, and W. Chen, "35.88 attenuation lengths and 3.32 bits/photon underwater optical wireless communication based on photon-counting receiver with 256-PPM," *Opt. Exp.*, vol. 26, no. 17, pp. 21685–21699, 2018.

[8] Y.-F. Huang, C.-T. Tsai, Y.-C. Chi, D.-W. Huang, and G.-R. Lin, "Filtered multicarrier OFDM encoding on blue laser diode for 14.8-Gbps seawater transmission," *J. Lightw. Technol.*, vol. 36, no. 9, pp. 1739–1745, May 2018.

[9] W. Lyu et al., "Experimental demonstration of an underwater wireless optical communication employing spread spectrum technology," *Opt. Exp.*, vol. 28, no. 7, pp. 10027–10038, 2020.

[10] Y. Chen et al., "26m/5.5 Gbps air-water optical wireless communication based on an OFDM-modulated 520-nm laser diode," *Opt. Exp.*, vol. 25, no. 13, pp. 14760–14765, 2017.

[11] X. Liu et al., "34.5 m underwater optical wireless communication with 2.70 Gbps data rate based on a green laser diode with NRZ-OOK modulation," *Opt. Exp.*, vol. 25, no. 22, pp. 27937–27947, 2017.

[12] H. M. Oubei et al., "4.8 Gbit/s 16-QAM-OFDM transmission based on compact 450-nm laser for underwater wireless optical communication," *Opt. Exp.*, vol. 23, no. 18, pp. 23302–23309, 2015.

[13] T.-C. Wu, Y.-C. Chi, H.-Y. Wang, C.-T. Tsai, and G.-R. Lin, "Blue laser diode enables underwater communication at 12.4 Gbps," *Sci. Rep.*, vol. 7, no. 1, pp. 1–10, 2017.

[14] M. Zhao et al., "Long-reach underwater wireless optical communication with relaxed link alignment enabled by optical combination and arrayed sensitive receivers," *Opt. Exp.*, vol. 28, no. 23, pp. 34450–34460, 2020.

[15] X. Ke and X. Xi, *Introduction to Wireless Laser Communication*, vol. 33. Beijing, China: Beijing Univ. Posts Telecommun. Press, 2004.

[16] F. Liu, M. Chen, W. Jiang, X. Jin, and Z. Xu, "Effective auto-alignment and tracking of transceivers for visible-light communication in data centres," *Proc. SPIE*, vol. 10945, pp. 134–141, 2019.

[17] J. Lin et al., "Machine-vision-based acquisition, pointing, and tracking system for underwater wireless optical communications," *Chin. Opt. Lett.*, vol. 19, no. 5, 2021, Art. no. 050604.

[18] J. A. Simpson, B. L. Hughes, and J. F. Muth, "A spatial diversity system to measure optical fading in an underwater communications channel," in *Proc. OCEANS*, 2009, pp. 1–6.

[19] A. H. Azhar, T.-A. Tran, and D. O'Brien, "A gigabit/s indoor wireless transmission using MIMO-OFDM visible-light communications," *IEEE Photon. Technol. Lett.*, vol. 25, no. 2, pp. 171–174, Jan. 2013.

[20] C. Chen, W.-D. Zhong, and D. Wu, "On the coverage of multiple-input multiple-output visible light communications," *J. Opt. Commun. Netw.*, vol. 9, no. 9, pp. D31–D41, 2017.

[21] T.-P. Ren, C. Yuen, Y. L. Guan, and G.-S. Tang, "High-order intensity modulations for OSTBC in free-space optical MIMO communications," *IEEE Wireless Commun. Lett.*, vol. 2, no. 6, pp. 607–610, Dec. 2013.

[22] Y. Song et al., "Experimental demonstration of MIMO-OFDM underwater wireless optical communication," *Opt. Commun.*, vol. 403, pp. 205–210, 2017.

[23] G. Xinyue and Z. Keer, "Research on STBC MIMO visible light communication system based on precoding," *Opt. Technol.*, vol. 45, pp. 436–442, 2019.

[24] S. M. Alamouti, "A simple transmit diversity technique for wireless communications," *IEEE J. Sel. Areas Commun.*, vol. 16, no. 8, pp. 1451–1458, Oct. 1998.

[25] L. Ma et al., "Experiments of recreating the frequency domain properties of seawater channel for underwater optical communication," in *Proc. OCEANS Marseille*, 2019, pp. 1–4.

[26] J. Guo, M. Fu, X. Liu, and B. Zheng, "Experiment-based channel characteristics for underwater wireless optical communication over medium-and-long distance," *Opt. Eng.*, vol. 62, no. 3, pp. 038107–038107, 2023.